

# An optically pumped silicon evanescent laser operating continuous wave at 60 °C

Hyundai Park, Alexander W. Fang, and John E. Bowers

Department of Electrical and Computer Engineering, University of California Santa Barbara, Santa Barbara, CA 93106  
[hdpark@engr.ucsb.edu](mailto:hdpark@engr.ucsb.edu)

Richard Jones and Mario J. Paniccia

Intel Corporation, 2200 Mission College Boulevard, SC12-326, Santa Clara, CA 95054

Oded Cohen

Intel Corporation, SBI Park Har Hotzvim, Jerusalem, 91031, Israel

**Abstract:** We demonstrate a silicon evanescent laser operating CW up to 60°C. The laser operates at 1568nm with a maximum fiber-coupled output power of 4.5mW. Devices are fabricated with silicon waveguides bonded to AlGaInAs quantum wells.

©2006 Optical Society of America

**OCIS codes:** (140.5960) Semiconductor lasers; (250.5300) Photonic integrated circuits

## 1. Introduction

Laser sources on a silicon platform are important for high level integration of photonic and electronic devices through CMOS VLSI processing. One big challenge of silicon-based active devices is poor light generation efficiency due to indirect bandgap characteristics of silicon. Efforts to overcome this hurdle have come in the form of a Raman Laser [1, 2] and LEDs [3] that utilize material engineering to increase the light emission efficiency of silicon. The work demonstrated here defines a mode by patterning a rib in the silicon waveguide while leaving the III-V quantum well region homogeneous across the wafer. With this approach, most of the optical mode is confined in the silicon waveguide providing high coupling efficiency with other passive silicon-based photonic devices while still achieving high optical gain through evanescent coupling into the III-V region. We recently demonstrated a silicon evanescent laser operating pulsed at 20 °C [4]. We report here a continuous wave silicon evanescent laser with a maximum operating temperature of 60 °C. At 20 °C, the uncoated devices operated up to 11 mW and the coated devices lase at 1568 nm with an optically pumped threshold of 23 mW and a maximum fiber-coupled continuous output power of 4.5 mW

## 2. Device Structure and Fabrication

The device structure is shown in Fig. 1a and the inset shows a scanning electron microscope (SEM) image of the structure. The device is divided into two regions: the silicon-on-insulator (SOI) passive-waveguide structure and the III-V active region that provides the optical gain. The SOI structure consists of a Si substrate, a 1 μm thick SiO<sub>2</sub> lower cladding layer, and a Si rib waveguide with a height (H) and rib-etch depth (D) of 0.7 μm and 0.6 μm respectively. The waveguide width (W) is varied from 1 μm to 5 μm. The III-V region consists of a two-period InP/1.1 μm InGaAsP super lattice (SL), a 110 nm thick InP spacer, a 50 nm thick unstrained 1.3 μm InAlGaAs separated confinement heterostructure (SCH) layer, strain-compensated AlGaInAs quantum wells, a 500 nm-thick unstrained 1.3 μm AlGaInAs SCH layer, and an InP upper cladding layer. The SL region employs 7.5 nm thick alternating layers of InP/InGaAsP to inhibit the propagation of defects from the bonded interface to the QW region [5]. Five 70 nm thick InAlGaAs quantum wells with compressive strain (0.85 %) and 100 nm-thick AlGaInAs barriers with tensile strain (-0.55 %) are used. The barrier layers have a bandgap corresponding to a wavelength of 1.3 μm.

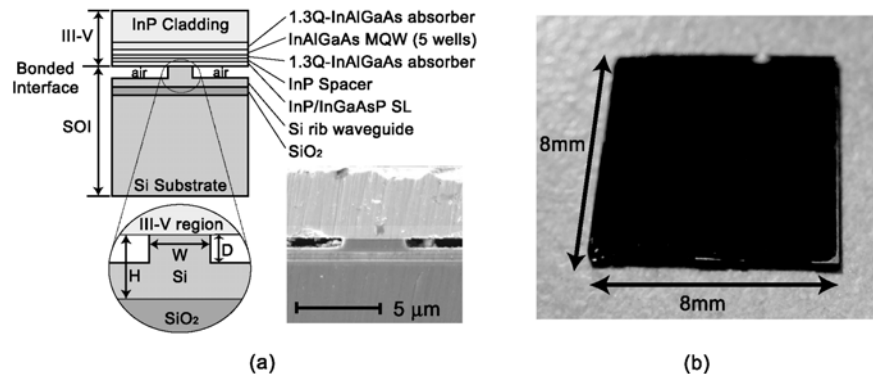


Fig. 1. (a) Device structure (inset) a SEM image, (b) AlGaInAs/Si SOI sample after InP substrate removal

Transverse confinement factors of silicon waveguides ( $\Gamma_{Si}$ ) are varied from 5 % to 51 % with waveguide width variation of 1  $\mu\text{m}$  to 5  $\mu\text{m}$  and correspondingly the QW transverse confinement factors ( $\Gamma_{QW}$ ) are varied from 5 % to 4 % for five quantum wells.

The silicon rib waveguide is fabricated on (100) surface of a lightly p-doped (doping concentration  $<2 \times 10^{15} \text{ cm}^{-3}$ ) silicon-on-insulator (SOI) substrate by standard photolithography and reactive ion etching (RIE) plasma of  $\text{Cl}_2/\text{HBr}/\text{Ar}$ . A thin layer of  $\text{SiO}_2$  was used as a hard mask. The SOI wafer and III-V epitaxial wafer are treated by buffered HF and  $\text{NH}_4\text{OH}$  respectively after a thorough cleaning procedure using acetone, isopropanol, and deionized water. The two samples are bonded together via oxygen plasma assisted bonding [6]. After a low temperature anneal ( $\sim 300^\circ\text{C}$ ), the InP substrate is removed with HCl. The devices are diced, the facets are polished, and the devices are characterized. Finally the facets are coated with a broadband dielectric HR coating ( $\sim 80\%$ ) consisting of three periods of  $\text{SiO}_2/\text{Ta}_2\text{O}_5$  and characterized again. The final device length after dicing and polishing is 800  $\mu\text{m}$ . An image of an  $8 \times 8 \text{ mm}^2$  bonded sample after InP substrate removal is shown in Fig. 1b. The bonded layer is continuous across the entire sample and is robust enough to stand up to dicing and polishing of the facets.

### 3. Experiment and Results

The device is optically pumped perpendicular to the laser by a 1250 nm fiber laser. The light from the pump laser is focused by a cylindrical lens illuminating a 12  $\mu\text{m}$  by 916  $\mu\text{m}$  rectangular spot incident on the device through the top InP cladding layer. The laser output is collected with a multimode fiber from the waveguide and subsequently characterized using a spectrum analyzer or photodetector. The fiber coupling efficiency is experimentally measured to be -5dB. The TE/TM near-field images of the output mode are recorded on an IR camera through a polarizing beam splitter and an 80x lens at the opposite waveguide facet.

Uncoated devices lase CW up to 35  $^\circ\text{C}$ . At 20  $^\circ\text{C}$ , the maximum power coupled into a single mode fiber is 11 mW. The remainder of this paper discusses the HR coated device results. Figure 2 shows the laser output power as a function of pump power and temperature for two different waveguide widths of 4  $\mu\text{m}$  and 1  $\mu\text{m}$ . In Fig. 2a, a 4  $\mu\text{m}$  wide device is operating with a threshold pump power of 23 mW and fiber-coupled maximum output power of 4.5 mW with a slope efficiency of 3 % at 20  $^\circ\text{C}$ . The total maximum output power taking into account the light from both facets and the coupling losses of -5 dB is approximately 28 mW and the corresponding slope efficiency is 16 %. The threshold increases from 23 to 105 mW between 20  $^\circ\text{C}$  and 60  $^\circ\text{C}$  and the structure exhibits a temperature coefficient ( $T_0$ ) of 27 K. The kinks in the LL curves are due to the multimode lasing with wide waveguide dimension. It is clearly shown from two different mode profiles in Fig. 2a that higher modes are superimposed with a fundamental mode at the region II of the LL curve while only a fundamental mode is lasing at the region I. Figure 2b shows LL curves of a 1  $\mu\text{m}$  wide device with a threshold of 120 mW and a slope efficiency of 0.5 % at 20  $^\circ\text{C}$ . Since this waveguide width is narrower, the fundamental mode is lasing without other higher order modes up to 0.6 mW. This device demonstrates a maximum fiber-coupled output power of 0.9 mW. The total maximum output power including the output from both facets and coupling losses is approximately 5 mW with a slope efficiency of 2.8 %.

In Fig. 3, the threshold pump power dependence on waveguide width is shown for different temperatures. The wider stripe lasers have lower threshold pump power than narrower devices because of low scattering losses and low propagation loss in the silicon waveguide.

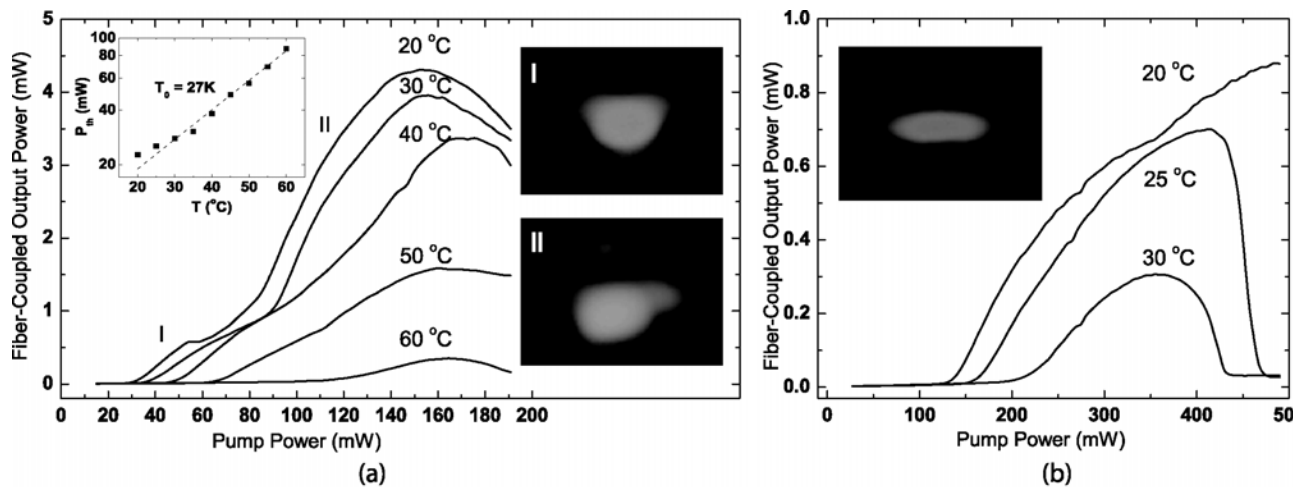


Fig. 2. LL curves and mode profiles (a) 4  $\mu\text{m}$  wide device (inset) threshold vs temperature (b) 1  $\mu\text{m}$  wide device

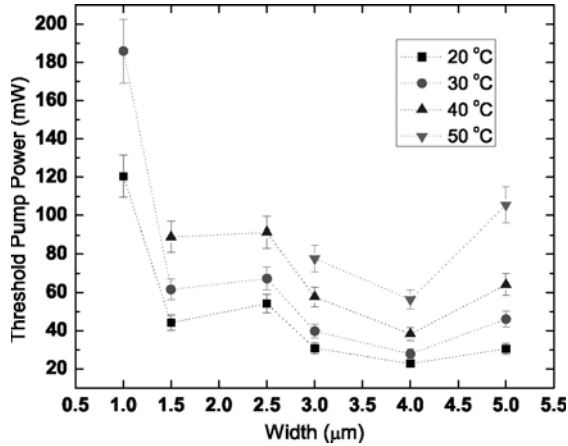


Fig. 3. Threshold pump power with different waveguide widths

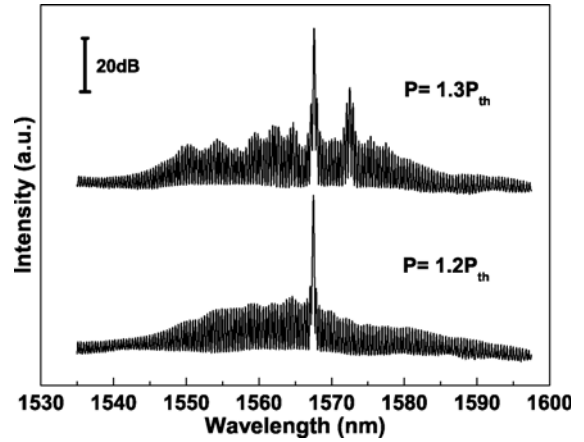


Fig. 4. Lasing spectra of a 4 μm wide device

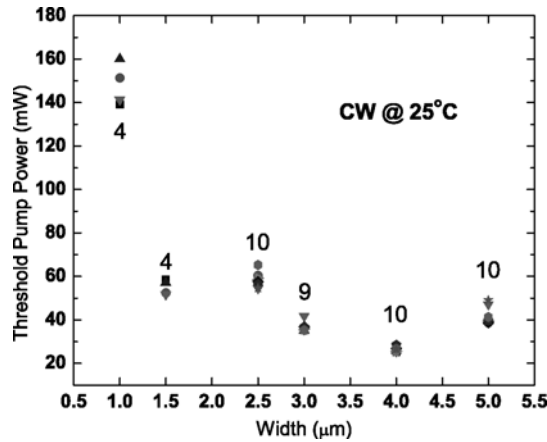


Fig. 5. Device yield and threshold variation. Number at each width represents the number of lasing devices out of 10.

Figure 4 shows the lasing spectrum of a 4 μm wide device with several pump powers all operating at 25 °C. The optical spectrum consists of the expected Fabry-Pérot response for the 800 μm long cavity, with a group index of 3.68. The calculated group index from simulations is 3.77.

Overall device yield and threshold variation are shown in Fig. 5. Sixty devices (ten devices at each of six widths) were characterized. 47 of the sixty devices are lasing with a variation of threshold power for each waveguide width of less than ±9 %. The yield of the four wider widths is 98%, but the yield is lower for the narrower stripe widths due to damage during polishing.

## 5. Conclusion

Continuous wave operation of an optically pumped silicon evanescent laser with maximum operating temperature of 60 °C is demonstrated. The laser consists of an AlGaInAs/InP active region bonded to a passive silicon rib waveguide. The laser has a threshold pump power of 23 mW and a maximum fiber-coupled output power of 4.5 mW operating at 1568 nm. The fabrication procedure includes standard CMOS compatible processing of the silicon waveguides and a low-temperature oxide-mediated wafer bonding process for heterogeneous integration. This process also provides good device yield with low performance variation. This work is a first step to integrate high performance active optical circuits with standard silicon compatible photonic devices. The technology should be extendable directly to enable electrically pumped lasers as well as other optically active devices including amplifiers, modulators, and photodetectors.

## 6. References

- [1] H. Rong *et al.*, "A continuous-wave Raman silicon laser," *Nature* **433**, 725, (2005).
- [2] O. Boyraz *et al.*, "Demonstration of a silicon Raman laser," *Opt. Express* **12**, 5269, (2004)
- [3] W. L. Ng *et al.*, "An efficient room-temperature silicon-based light-emitting diode," *Nature* **410**, 192, (2001)
- [4] A. W. Fang, *et al.*, "An optically pumped silicon evanescent laser," *ECOC 2005*, Post Deadline, 2005.
- [5] A. Karim *et al.*, "Super lattice barrier 1528-nm vertical-cavity laser with 85°C continuous-wave operation," *IEEE Photon. Technol. Lett.* **12**, 1438, (2000)
- [6] D. Pasquariello *et al.*, "Plasma-Assisted InP-to-Si Low Temperature Wafer Bonding," *IEEE J. Sel. Topics Quantum Electron.* **8**, 118, (2002)